Acta Geochim (2022) 41(5):811–822
https://doi.org/10.1007/s11631-022-00543-0

ORIGINAL ARTICLE

Genesis and soil environmental implications of intact *in-situ* rhizoliths in dunes of the Badain Jaran Desert, northwestern China

Qingfeng Sun[1,2] · Kazem Zamanian[3,8] · Arnaud Huguet[4] · Omid Bayat[5] · Hong Wang[6] · Hanan S. Badawy[7]

Received: 25 January 2022 / Revised: 5 April 2022 / Accepted: 18 April 2022 / Published online: 4 August 2022

Abstract
Desert rhizoliths are generally found as weathered, broken and scattered samples on dune field surface, but rarely *in-situ* in their initial states buried under the soil of desert in the Badain Jaran Desert, northwest China. This study offers an assessment of the morphological, mineralogical, and chemical properties of intact and *in-situ* rhizoliths found in soils of swales and depressions among dune chains. The characteristics of these rare and precious objects were assessed using optical polarizing microscopy, cathodoluminescence, scanning electronic microscopy, radiocarbon dating, and stable isotopic analyses, providing the opportunity for discussion of the rhizolith formation mechanisms and associated environmental conditions. Field and laboratory investigations showed that the *in-situ* intact rhizoliths were formed only in the places where *Artemisia* shrubs are living, and the remaining root relicts within rhizoliths belong to this species. The spatial distribution of rhizoliths also suggested that low topographic positions on a landscape provided soil moisture, and redox environments favored rhizolith formation. A semi-closed redox environment in the subsoil at swales and depressions, where water is always present, along with the sandy soil texture, facilitated fast water percolation to deeper depths and condensation. Such a soil environment not only provides water for *Artemisia* growth, but also for the weathering of minerals such as felspars and calcite from primary carbonates, and for the decomposition of root relicts. Furthermore, harsh climatic conditions, such as strong winds and solar radiation, led to water evaporation through dead root channels and triggered the calcification along the root relicts. The entrapped lithogenic carbonates and to a lesser extent the decomposition of *Artemisia* roots provided the carbon sources for the rhizoliths formation, while the weathering of soil minerals, particularly feldspars and carbonates, was the main source of Ca. Rhizoliths in the Badain Jaran desert formed relatively quickly, probably over a few soil drying episodes. This led to the entrapment of a large quantity of lithogenic carbonates (more than 90% of carbon) within rhizolith cement. The re-dissolution of the entrapped lithogenic carbonates in rhizolith tubes should be taken into account in the paleoenvironmental interpretation of ^{14}C ages, the latter suggesting that rhizoliths formed during the Holocene (~2053 years cal BP, based on root organic relicts).

Keywords Rhizoliths · Calcification · Leptic regosols · *Artemisia* roots · Decomposition · Soil moisture

✉ Qingfeng Sun
sqf@nwnu.edu.cn

✉ Kazem Zamanian
zamanian@ifbk.uni-hannover.de

1 Key Laboratory of Resource Environment and Sustainable Development of Oasis, Northwest Normal University, 730070 Lanzhou, Gansu Province, Gansu, PR China

2 Key Laboratory of Eco-function Polymer Materials of the Ministry of Education, Northwest Normal University, 730070 Lanzhou, Gansu, PR China

3 Institute of Soil Science, Leibniz University of Hannover, Herrenhäuser Straße 2, 30419 Hannover, Germany

4 Sorbonne Université, CNRS, EPHE, UMR METIS, F-75005 Paris, PSL, France

5 Department of Soil Science, Isfahan University of Technology, 84156-83111 Isfahan, Iran

6 Interdisciplinary Research Center of Earth Science Frontier, Beijing Normal University, 100875 Beijing, PR China

7 Department of Geology, Faculty of Science, Beni-Suef University, 62521 Beni-Suef, Egypt

8 School of Geographical Sciences, Nanjing University of Information Science and Technolog, 210044, Nanjing, China

1 Introduction

Soil is at the heart of the Earth's critical zone (Chorover et al. 2007). Biomineralization, including pedogenic carbonate

formation, is a common feature of soil evolution. It occurs not only in soil but also around or within roots, separately or concomitantly. Carbonate rhizoliths are one type of pedogenic carbonates (Lambers et al. 2009) where mineralization takes place around roots in modern (Holocene) soils and paleosols (Sun et al. 2019a, b, 2020; Huguet et al. 2020; Brazier et al. 2020).

Rhizoliths are generally defined as ichnofossils (root traces) or fossils (petrified roots) in geology, taphonomy, and paleontology (Kraus and Hasiotis 2006; Barta, 2011). Phytocretions (minerals precipitate form an external mold of a plant, other than the root. Liutkus 2009) are similar to rhizoliths and formed around plant stem in standing water above sediments. In arid environments, the fluctuations in water table levels, pedogenesis, and erosive dynamics expose the plant remains to subaerial weathering, resulting in low rates of preservation of plant macrofossils (Gastaldo and Demko 2011) and explaining the rare presence of intact rhizoliths in such settings. However, rhizoliths are important indicators of paleo- and modern plants (Nascimento et al. 2019), especially in desert soils. Rhizoliths can be used as environmental markers of humidity, drainage, and local topography (Kraus and Hasiotis 2006; Li et al. 2015).

The formation mechanisms of rhizoliths have been widely discussed (e.g., Liutkus et al. 2005; Kraus and Hasiotis 2006; Owen et al. 2008; Gocke et al. 2010, 2011, 2014; Bojanowski et al., 2016 ; Li et al. 2015a, b; Nascimento et al. 2019; Golubtsov et al., 2019) and remain open to question. This is partly due to the difficulties involved in probing the rhizosphere – the microscale environment immediately surrounding root tissue, and also due to the numerous factors which can affect rhizoliths formation. Such factors include, for example, the nature of the cementing mineral, soil humidity and microbial activity (McLaren 1995), root exudation of organic acids (Albalasmeh and Ghezzehei 2014; Marschner 1995), mass-flow (Cramer and Hawkins 2009) and evaporative concentration and evapotranspiration (Owen et al. 2008). Moreover, other factors like the interplay of organic matter, bio-chemicals of production and/or decomposition of living and/or deceased organic tissues, mineral weathering, mineral-water-root interfaces, redox conditions, microorganism, gas exchange, pH, as well as soil physical properties can also affect rhizolith formation (Zhao et al. 2020; Dontsova et al. 2020; Liang et al. 2018; Dwivedi et al., 2017; Spohn et al. 2013; Sanaullah et al. 2011; Jones et al. 2009; Smits et al. 2005; Rasse et al. 2005; Hinsinger et al. 2003; Der Hoven and Quade 2002; Van Breemen et al. 1983). It is therefore challenging to determine the formation mechanisms of rhizoliths, which form in different sedimentary and diagenetic environments (Sun et al. 2019b).

Rhizoliths in the deserts of northwest China have been widely studied (Li et al. 2015a, b, 2017; Sun et al. 2019a, b) and have been observed either at the soil surface or sub-surface. The surficial rhizoliths are most commonly eroded out of dune soil and weathered at the soil surface, where they are subjected to late or epi-diagenesis like wind erosion, dissolution, radiation, and physical thermal expansion and cold contraction. This results in the fragmentation of rhizoliths at the soil surface (Li et al. 2015a, b, 2017; Yang 2000; Chen et al. 2004; Gao et al. 1993), modifying the original characteristics of the rhizoliths associated with their formation underground. Here, we term "*in-situ* rhizoliths (IR)" the rhizoliths preserved vertically and deeply underground and which were not subject to any weathering and epidiagenetic process, in contrast with the reworked and weathered rhizoliths (EWR). To date, pristine rhizoliths from deserts have only been investigated at one site (Tengeri Desert, NW China) (Sun et al. 2020), where they were observed to be preserved horizontally within shallow subsurface dune soils. The pristine rhizoliths from the Badain Jaran deserts differ from those of the Tengeri Desert, as they are positioned vertically within the deep Holocene soils stratigraphy (Fig. 1a, b). These two types of pristine rhizoliths – horizontal- or vertical- – might have different mechanisms of formation, potentially related to contrasting environmental settings. In the present study, the pristine rhizoliths from the Badain Jaran Desert were characterized using field observations as well as microscopic and isotopic techniques to elucidate their formation mechanisms.

2 Geographical setting

The Badain Jaran desert, at an altitude of 1,200–1,700 m a.s.l., is characterized by the co-existence of mega-dunes and lakes (Ma and Edmunds 2006; Yang et al. 2011; Jiao et al. 2015; Shao et al. 2015; Zhang et al. 2017). The heights of the mega-dunes are usually 200–300 m and can reach over 500 m in its southeastern part (Dong et al., 2013). The annual precipitation is 40–120 mm and mainly occurs in summer. The annual potential evaporation is over 2500 mm with mean annual air temperatures from 9.8 to 10.2 °C. The mean annual surface wind speeds range from 2.8 to 4.6 $m \cdot s^{-1}$, and the dominant wind directions are northwest and west (Dong et al. 2004; Zhang et al. 2017). The precipitations which are < 5 mm account for approximately 90% of all rain/snow events in the desert and evaporate from the mega-dune surface in 1–3 days (data from the recent fifty years; Ma et al. 2014 and 2017). Our investigations over the last years showed that the vegetation in the southeastern margin of the desert is mainly constituted of *Artemisia*, *Psammochloa*, and *Phragmites* species. They are mainly

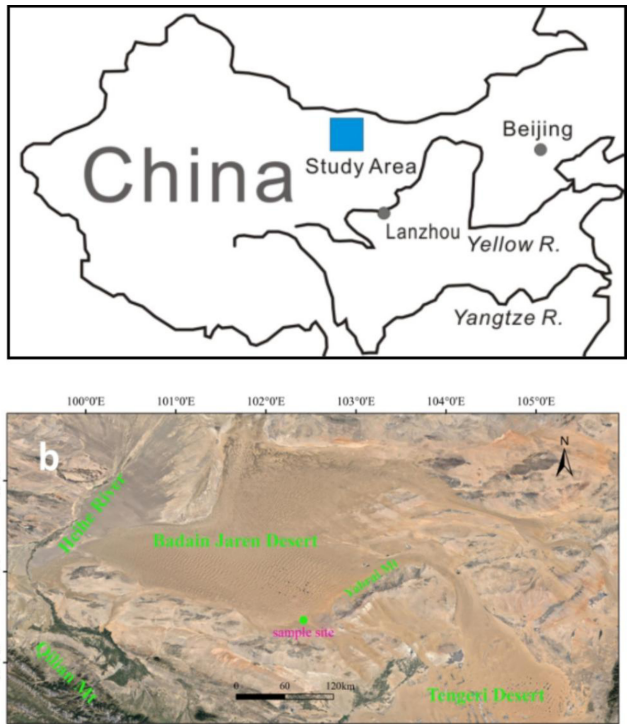

Fig. 1 Locations of the study area and the sampling site
a: Location of the Badain Jaran Desert, northwestern China
b: Location of sampling site of rhizoliths in the southeastern margin of the Badain Jaran Desert

present in the lowermost portions of the landscapes, i.e. swales and depressions between the dunes in the deserts of NW China.

The dune soils contain primary and secondary rock and mineral debris from outside of the deserts and the local weathered bedrocks by wind transportation and mixture, and the average carbonate content of the soils is 6.47 % (Sun et al. 2019a). Previous works also confirmed that carbonate minerals are present in low amounts in the silicate desert sands based on XRD analysis (Gates et al. 2008; Bai 2011). The calcium carbonate content is between 0.5 % and 2.5 % by weight in the dune sands of the Badain Jaran Desert (Li and Yang 2004). The average carbonate content of the Badain Jaran desert is 4.64% (Wang et al. 2004), while it can be as high as 23% in the calcareous layers in these deserts (Yang et al. 2003). It is sufficiently large to impact the radiocarbon ages of dune sediment (Yang et al. 2010) and rhizolith carbonate cement. Soil carbonates formed through cycling generations with a mixture of lithogenic and pedogenic pre-carbonate, as well as new-formed carbonate from weathered silicates (Monger 2014; Monger et al. 2015).

3 Materials and methods

In the vast area of the Badain Jaran desert, EWR are commonly scattered due to erosion and weathering on dune soil surfaces. In contrast, IRs were only found at one place in the southeastern peripheral margin of the desert. Therefore, rhizoliths were investigated and collected from five sites in an area of the margin (Fig. 2a, ~39°28′N, ~102°26′E). EWR occurred in the swales between small dunes (Fig. 2b). A pit of about 50 cm depth was carefully excavated around IR (Fig. 3a) until it was entirely exposed (Fig. 3b, c, d). The petrographic and mineralogic analyses of one IR specimen were carried out in the laboratory of the Northwest Petroleum Institute, Lanzhou, China. The specimens were first impregnated with resin, cut into transverse sections, and polished to 4.8 cm × 2.8 cm slices. A Zeiss Scope A1 microscope was used to examine the mineral crystal morphology under transmitted plain light. The technique of Dickson (1966) was applied to stain the calcareous cement of the rhizoliths, with alizarin red-S allowing to discriminate between calcite and dolomite, and then a mixture of potassium ferricyanide and alizarin red-S indicating the presence of ferroan or non-ferroan calcite and/or ferroan dolomite. The luminescence pattern of the grains and cement forming the studied rhizoliths was investigated by cathodoluminescence (CL) with a CITL CL8200 MK5 instrument. A fragment of IR rhizolith was gold coated, and then analyzed using an FEI Quanta 450 scanning electron microscope (SEM) coupled with an energy dispersive X-ray spectrometer (EDX) to examine the ultra-microscale features and the chemical composition of the cement.

The radiocarbon dating and isotope analyses were performed at the Guangzhou Institute of Geochemistry, Chinese Academy of Sciences. The EWR tubes with root hairs (Fig. 3e), the IRs with root relicts, and the root hairs (Fig. 3e) were radiocarbon dated. They were treated using the standard acid-alkali-acid method (Shen et al. 2010). The samples were firstly smashed into small pieces, and then cleaned and washed with ultrapure water (MilliQ, Millipore) in an ultrasonic bath before being treated with phosphoric acid (~ 100%). The CO_2 gas resulting from this treatment was purified in a vacuum line and finally sealed into a reaction tube for graphitization (Xu et al. 2007). The graphite was measured with a 0.5 MeV compact accelerator mass spectrometry (National Electrostatics Corporation, 0.5MV 1.5SDH-1 AMS). The precision of the measurement is close to 2‰. The data were corrected for isotopic fractionation using online AMS $\delta^{13}C$ values. All the radiocarbon ages were calibrated into cal BP using Intcal20.^{14}C (Reimer et al. 2020) (Table 1). Root samples and other parts of fresh plant tissue were treated in the traditional way (acid-alkali-acid treatment). Samples were dried in a freeze dryer.

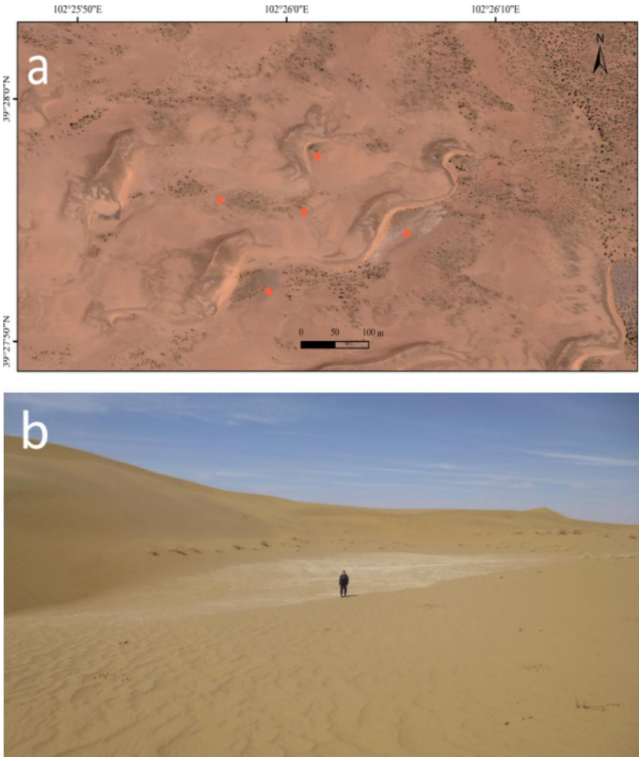

Fig. 2 Geomorphology of sampling sites of the studied rhizoliths
a: General view of the studied area and sampling sites (red dots) of the EWRs that occur in swales and depressions between dune chains. *Artemisia* shrubs are sparsely scattered in the swales and depressions (fine black dots)
b: Whitish broken rhizotubes of scattered EWRs look like frost or snow from far away. The black dots on the slope of dunes in the far distance are *Psammochloa* herbs

Subsamples were split up into quartz tubes in the presence of copper oxide and silver wire. The quartz tubes were pumped to 1.0×10^{-3} torr in a vacuum line and then sealed using a torch. The sealed tubes were placed into an oven at 900 °C for organic carbon oxidation. The $\delta^{13}C$ and $\delta^{18}O$ values of the carbonate cement of five rhizoliths and three *Artemisia* plant specimens were also determined separately using an isotope ratio mass spectrometer (Thermo Finigan Delta Plus XL; Table 2).

Soil paleotemperatures derived from rhizolith carbonates were calculated using the following equation developed by Dworkin et al. (2005) based on the database of the Holocene carbonates (Cerling and Quade 1993):

$$\delta^{18}O = 0.49 \times MAAT - 12.65$$

where $\delta^{18}O$ and MAAT represent the oxygen isotopic composition of the carbonate (‰), Pee Dee Belemnite (PDB) and the mean annual air temperature (°C), respectively. This equation is suitable for carbonates with $\delta^{18}O$ values comprised between −13‰ and −1‰ (PDB). The values outside this range reflect post-formation processes (e.g. diagenesis, recrystallization) or evaporative enrichment (Dworkin et al. 2005).

4 Results

4.1 Field observations on rhizoliths and host soils

The eroded and weathered rhizoliths (EWRs) were found in the swales and depressions between dune chains (Fig. 2a). The whitish broken rhizotubes (Fig. 3a) were exhumed by wind erosion and looked like frost or snow from distance (Fig. 2b). *Psammochloa* herbs (Fig. 2a) and *Artemisia spp*. shrubs (Fig. 3a) occurred sparsely in the swales and depressions (Fig. 2a).

Only the vertical rhizoliths preserved in sand soil were expected to be pristine, *in-situ* rhizoliths (IR). Only five IRs were found in an area of about 20×20 m^2 in a swale where EWRs were also present (Fig. 3a). One vertical rhizolith was extracted for detailed examination in the present study. Wind striations were visible across the pit wall (Fig. 3b) and on the rhizoliths (Fig. 3c). The soil was dry at the surface (Fig. 3a, b, c) and moist below 10–15 cm depth (Fig. 3b) and can be classified as Leptic Regosols (FAO, 2014).

The underground part of the IR was much thicker and more fragile than the aboveground part (Fig. 3c). The central part of the IR corresponds to a hollow channel filled with root residuals and sand (Fig. 3d). The halo around this central part is whitish to yellow-brown and becomes grey-beige with distance from the center (Fig. 3d).

The EWRs appeared as small whitish broken tubes densely and randomly scattered at the soil surface (Fig. 3a). Hair-like root relicts were found within one EWR (Fig. 3e). The hollow channel of the EWR was also made of brown root remains mixed with sand (Fig. 3f).

4.2 Petrography

Microscopically, the IR consists of poorly cemented grains, mainly of quartz, but also feldspars, and carbonates that are stained brownish-red with Alizarin red-S (Fig. 4a). The lithogenic carbonates or primary carbonates particles originate from windblown materials from around the desert bedrocks (Sun et al. 2019a) and appear as patches or lumps (Fig. 4a). The grains are entrapped by micritic calcareous cement with no sign of post-diagenetic alteration (Fig. 4a).

Cathodoluminescence analyses (Fig. 4b) confirmed the nature of the clastic grains of the rhizoliths, with quartz grains in dark brown-blue (Mavris et al. 2012; Omer 2015), feldspars in blue (alkali feldspar) or green (plagioclase) (Scholonek and Augustsson 2016), and lithogenic carbonates in orange (Omer et al. 2014; Kolchugin et al. 2016).

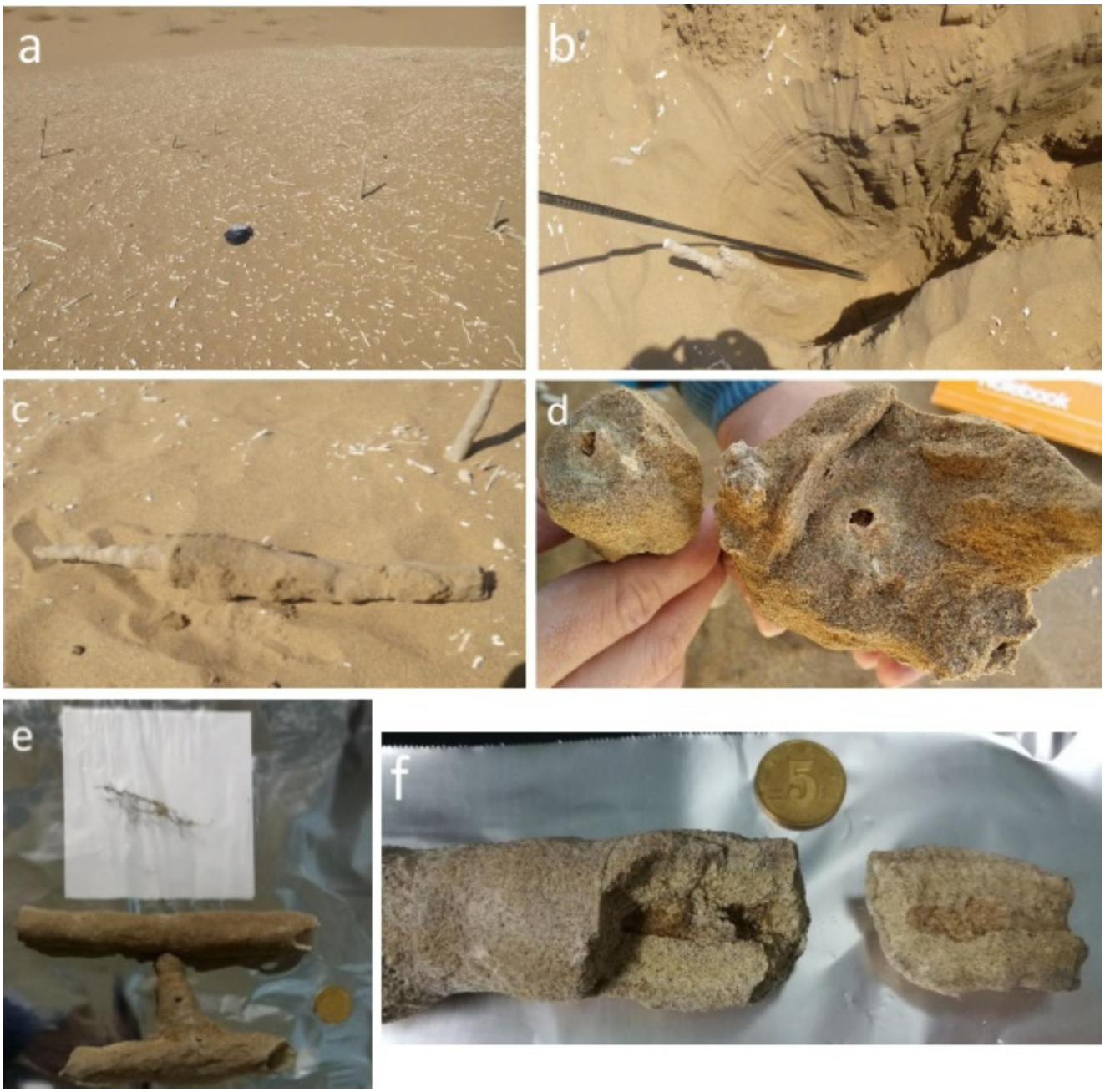

Fig. 3 Field characteristics of the rhizoliths
a: White weathered and broken rhizoliths are horizontally scattered on the soil surface. A few vertically standing rhizoliths can also be observed. The small shrubs in the left upper corner are *Artemisia spp.* (the black camera bag is 8 cm×12 cm)
b: *In-situ* rhizoliths found in a ca. 50 cm-deep pit. The dune soil is wet at depth and the sand-stratification was clear
c: The underground part of the rhizoliths (of Fig. 3b) is much thicker than the eroded and weathered part. The rhizolith shows clear sand-stratification
d: Root relicts inside the central hollow and a white halo within the IR (of Fig. 3c) after having been broken. The relicts were radiocarbon dated
e: Root hair relicts and rhizoliths. The relicts were pulled out of the EWR and were radiocarbon dated (the coin diameter is 20 mm)
f: Brown root remains were mixed with soil within an EWR (the coin diameter is 20 mm)

The carbonate cement is recognizable as bright orange dots scattered among clastic grains (Fig. 4b). The cement consists of low magnesium calcite (Fig. 4c, d).

4.3 Radiocarbon ages

The results of radiocarbon dating of the IR (Fig. 3d) and EWR (Fig. 3e) specimens are shown in Table 1. The age of the organic relicts in the central hollow channel of the IR is

Table 1 AMS radiocarbon ages of rhizoliths in the Badain Jaran Desert

Sample (Lab) No./ rhizolith type	Position	Material	AMS $\delta^{13}C$	$F^{14}C$	±1 σ	Age (^{14}C yr BP)	±1 σ	$\Delta^{14}C$	±1 σ	Age (Cal BP)	±1 σ
8453/IR	G-2	carbonate cement	-2.1	0.3754	0.0014	7870	35	627.6	1.4	8628	32
8457/IR	G-2	root relicts	-17	0.7708	0.0020	2090	25	235.4	2.0	2053	16
8454/EWR	E	carbonate cement	-2.0	0.5714	0.0013	4495	20	433.2	1.3	5232	19
8458/EWR	E	root relicts	-24	1.0444	0.0017	-345	15	36.0	1.7	2009 CE	

Note: BP: Before present, defined as before 1950; $F^{14}C$: Fraction of modern carbon; Cal: Calibrated using CALIB7.1 for BP and CALIBomb for C.E. age; IR: *in-situ* rhizoliths; EWR: Eroded out and weathered rhizoliths; CE: common era

2053 ± 16 years cal BP. The root hair relicts within the EWR are modern in age (2009 C.E.). The age of the EWR cement is 5232 ± 19 years cal BP and the IR cement is 8628 ± 32 years cal BP.

4.4 Stable carbon and oxygen isotopes

The $\delta^{13}C$ and $\delta^{18}O$ values of the carbonate cement and the carbonate particles of rhizoliths and *Artemisia spp*. tissues were shown in Table 2. The mean $\delta^{13}C$ (VPDB) and $\delta^{18}O$ (VPDB) values of the EWR cement are −2.6‰ and −6.8‰, respectively. Similar values were observed for the IR cement, with $\delta^{13}C$ and $\delta^{18}O$ values of −2.5‰ and −6.2‰. *Artemisia* tissues are characterized by $\delta^{13}C$ and $\delta^{18}O$ values of -26.7‰ to -28.5‰ and − 27.4‰ to -32.1‰, respectively.

5 Discussion

5.1 Ages of rhizoliths, stable isotopic composition and environmental implications

Modern analogs of initial biomineralization around plant roots are rare (Alonso-Zarza 2018). However, some root relicts were radiocarbon dated to Holocene in modern loess (Gocke et al. 2011), aeolian sand dunes (Cramer and Hawkins 2009), coastal/inland sands (Joseph & Thrivikramaji, 2005), and bay dunes (Rao and Thamban 1997). Apparent carbonate radiocarbon ages (Table 1) indicate that the rhizolith formation in the Badain Jaran Desert occurred during the Holocene (8–2 ka ago).

The $\delta^{13}C$ values of the *Artemisia* tissues (−26.74‰ to −28‰, Table 2) confirm the C_3 nature of *Artemisia* (Liu et al. 2017) because the C_3 photosynthesis pathway occurs in most shrubs, herbs, and (cool-season) grasses with $\delta^{13}C$ values ranging between ~ −25‰ and ~ −32‰ (Vogel 1993; Basum et al. 2015), with a mean value of −27‰ (Smith and White 2004; Basum et al. 2015). Generally, C_3 plants in arid environments present slightly higher $\delta^{13}C$ values than those from temperate regions (Cerling and Quade 1993; Zamanian et al., 2021). When the fluxes of CO_2 derived from organic matter decomposition in soils are higher than the rates of pedogenic carbonate formation, the $\delta^{13}C$ values of secondary carbonates are mainly controlled by those of soil CO_2 and they can be used as an indicator of the local vegetation cover (Cerling 1984; Cerling and Quade 1993; Quade 2014), after adjustment for isotopic fractionation and diffusion. Rhizoliths form in isotopic equilibrium with root-derived C (Gocke et al. 2011) and their $\delta^{13}C$ values are generally enriched by about 14‰ to 16‰ related to the root-derived C (Cerling 1984; Cerling and Quade 1993; Zamanian et al. 2016a). In the present study, the difference between the $\delta^{13}C$ values of *Artemisia* tissues (ca. −27‰) and rhizoliths (about −2‰ to −3‰) (Table 2) is much larger than 14−16 ‰. Logically and theoretically, there are three possible explanations for this difference: (1) rhizoliths originate from other plant species than *Artemisia*, with a C_4 metabolic pathway; (2) rhizoliths were subjected

Table 2 $\delta^{13}C$ and $\delta^{18}O$ stable isotope values of rhizoliths cement and *Artemisia* tissues in the Badain Jaran Desert

Rhizolith/Root Type		Sample No	Position	Material	$\delta^{13}C_{V-PDB}$ (‰)	$\delta^{18}O_{V-PDB}$ (‰)	Paleotemperature(˚C)
EWR (cement)		DM-A	A	Carbonate	-2.42	-7.22	10.92
		DM-B	B	Carbonate	-3.02	-7.24	10.70
		DM-E	E	Carbonate	-2.43	-5.96	13.46
		average			-2.62	-6.81	11.75
IR (cement)		DM-G-1	G	Carbonate	-2.53	-6.90	11.57
		DM-G-2	G	Carbonate	-2.44	-5.58	14.22
		average			-2.49	-6.24	12.89
Artemisia tissues	Dead root	A-1	A	Carbon	-26.74	-27.38	
	Fresh stem	A-2	A	Carbon	-28.47	-28.70	
	Fresh seedling	A-3	A	Carbon	-28.30	-32.05	

Note: V-PDB: Vienna-Pee Dee Belemnite

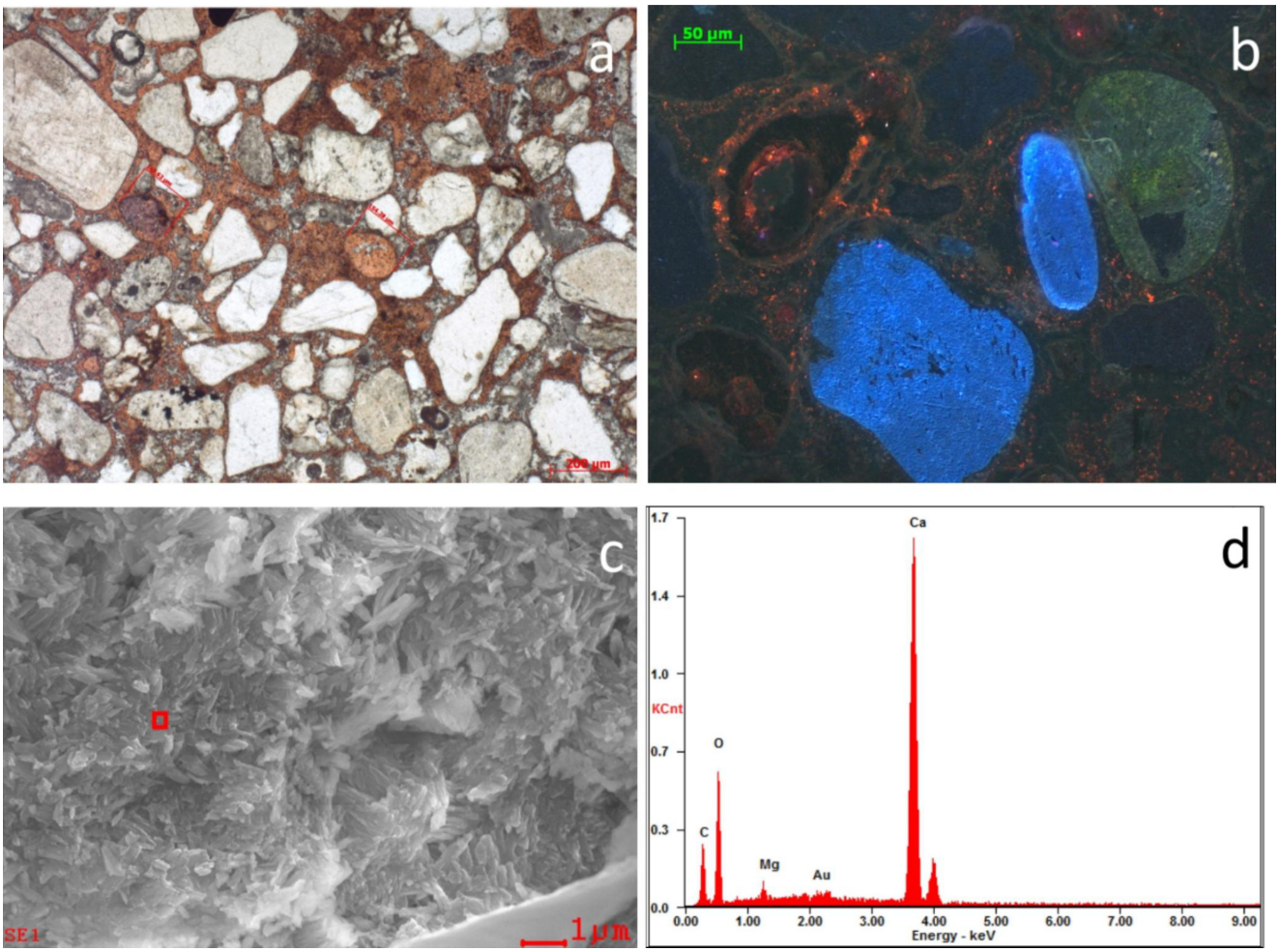

Fig. 4 Microscopic features of the studied rhizoliths
a: Clastic particles and stained cement of an IR under microscope. Most of the particles are quartz (white), but a small amount of feldspar (gray) and carbonate rock fragments are also present. Two carbonate particles (marked by red lines) were stained in brown/red. The image was taken under plane-polarized light;
b: Round clastic particles surrounded by cement viewed by cathodoluminescence. The light blue and green grains are feldspars; the deep dark grains are quartz. The small red-orange dots are carbonate cement. The other parts showing no luminescence correspond to carbonate cement covered by clay minerals. The dark color of cement can also be due to the addition of Fe^{2+} and Mn^{2+} cations during rhizolith formation in a weak redox environment. In the upper-left corner of the picture, the dotted orange loop-like halos may be calcite derived from the weathered feldspar grains (plane-polarized light);
C: Crystalline structure of rhizoliths calcite cement under SEM;
D: EDX spectroscopy of the marked area in Fig. 4c shows that the mineralogy of rhizolith cement is calcite or low Mg calcite.

to diagenetic processes, such as wind erosion, dissolution, radiation, physical thermal expansion, and cold contraction on the soil surface; (3) there was a large contribution of lithogenic carbonates due to relatively fast formation of rhizoliths in the Badain Jaran desert.

The first hypothesis can be rejected, as field observations clearly showed the close association between rhizoliths and *Artemisia* plants (Figs. 2a and 3a). Similarly, the second one can be excluded, as microscopic analyses revealed no diagenetic changes in the rhizoliths carbonates (Fig. 4a, b, c). Therefore, the third hypothesis is the most likely and is also supported by a large age discrepancy between root remains and the rhizolith cement (Table 1). A mixture of secondary/pedogenic and lithogenic carbonates in rhizolith cement and also diffusion of atmospheric CO_2 in soils with low rates of respiration can lead to enrichment in $\delta^{13}C$ values. Amundson et al. (1989) found that a low density of vegetation cover was the main reason for the entrance of atmospheric CO_2 (with $\delta^{13}C$ values ~ -6.5‰ for pre-industrial CO_2) into soils and enrichment of $\delta^{13}C$ values in the pedogenic carbonates of the Mojave Desert, California. The enrichment of $\delta^{13}C$ values of secondary carbonates was also observed in the deserts of central Iran, which was related to a decline in the vegetation cover and influx of atmospheric CO_2 over

time (Bayat et al. 2018). Therefore, the lithogenic carbonate residues inside the rhizoliths of the desert can explain the enrichment of $\delta^{13}C$ values. Furthermore, sparse vegetation density in the Badain Jaran desert (Dong et al. 2004; Zhang et al. 2017), low respiration rates, and a sandy texture of the soil (Figs. 2b and 3b) lead to infiltration of atmospheric CO_2 and can further enhance this enrichment.

The $\delta^{18}O$ value of secondary carbonates was shown to be related to the $\delta^{18}O$ value of local meteoric water which is controlled by air temperature and evaporative conditions (Cerling 1984; Cerling and Quade 1993; Quade 2014; Zamanian et al., 2021). As ^{14}C dating of carbonates shows that rhizoliths were formed during the Holocene (Table 1), we applied an empirical model for paleotemperature reconstruction based on Holocene carbonates (Dworkin et al. 2005). The reconstructed temperatures from rhizoliths of the Badain Jaran desert (Table 2) are ca. 2 to 3 °C higher than the mean annual temperature recorded in the region (Dong et al. 2004; Zhang et al. 2017). However, the analyzed rhizoliths consist of a large contribution (more than 90%) of lithogenic carbonates from our pre-studies (Sun et al. 2019a) that challenges the reliability of any paleo-environmental reconstructions based on rhizoliths for Badain Jaran desert, even though the determined paleo-environmental information looks reasonable.

5.2 Mechanism of rhizolith formation in dune soil of Badain Jaran desert

There are two potential sources of Ca^{2+} for calcification of the initial intact rhizoliths in the Badain Jaran desert: (i) dissolution of the lithogenic carbonates of dune clastic particles transported by the wind; (ii) weathering of other minerals like feldspars (e.g. plagioclases) (Fig. 4b; Gudbrandsson et al. 2014). The release of organic acids via organisms during root decomposition increases the dissolution rate and solubility of silicate minerals like feldspars (Welch and Ullman 1996), which releases calcium cations. The mechanisms of feldspar dissolution and weathering are subjects of discussion (Yuan et al. 2019). Nevertheless, the weathering rates of feldspars were shown to be proportional to their exposed surface areas (Holdren and Speyer 1985) and the population of surface complexes with H^+, OH^- or ligands (Bloom and Nater 1991).

When the root dies, it can still provide a conduit for downward and upward percolation of solutions and air. This leads to the dissolution of carbonates and minerals weathering as well as carbonates re-precipitation within or around the decaying roots, which forms a petrified root tubule (Sarjeant 1975; Nascimento et al. 2019). Calcite can precipitate along the root hollow channel due to the steep chemical gradient occurring around the dead root. The formation of calcite in and around roots is favored by the episodic drying phases of the soil, which often occurs in deserts due to strong solar radiation and wind (Cohen 1982; Kraus and Hasiotis 2006). These episodic drying events prevent the complete dissolution of lithogenic carbonates, but the entrapment in the rhizolith cement (i.e. the pedogenic carbonate). This formation procedure points to the fact that rhizoliths form relatively fast, over a few drying events, and even after root death. Furthermore, the sandy structure of the soil facilitated cementation with a relatively small amount of precipitated pedogenic carbonates. The specific fast formation and incomplete recrystallization of carbonates (Zamanian et al. 2016b and c) in equilibrium with respired CO_2 make the studied rhizoliths in Badain Jaran Desert inappropriate for paleo-environmental reconstructions and radiocarbon dating. This is in contrast with many recently published works that suggest the suitability of rhizoliths for paleo-environmental reconstruction (Gocke et al. 2010, 2011, 2014; Bojanowski et al. 2015; Li et al. 2015a, b; Nascimento et al. 2019).

Soil moisture is a key factor in the rhizolith formation process. Rhizolith formation around decaying roots needs a semi-closed, weak redox environment (Fig. 5). Indeed, both shallow dry, and deeper waterlogged soils are not favorable environments for root decomposition and associated CO_2 production, as an open and dry environment prevents root decay, while closed reducing environments lead to organics fermentation and CH_4 production rather than HCO_3^- (Sun et al. 2019a). The homogenous porous sandy soil of the Badain Jaran Desert (Fig. 3a, b) and the harsh climatic condition of the region provide a favorable condition in terms of soil moisture, i.e., episodic wetting and drying cycles. Soil moisture is further controlled by landscape geomorphology. The desert vegetation is solely distributed at the foot of dunes (Fig. 2a, b) on the beds of swales and depressions, where rainwater accumulates and underground pore water migrates from higher landscape positions. In the depressions, the Ca^{2+} concentration also increases (Bai 2011), which further favors rhizolith formation.

In the Badain Jaran Desert, IRs are progressively eroded out of dune soils and become thinner due to wind and weathering, forming the EWRs. Some features of the former roots, such as root hairs within the hollow channels of the EWR (Fig. 3d, e), can still be preserved because of extreme aridity at the surface and also protection offered by the rhizolith carbonate cement. Nevertheless, fine roots are rarely found within the EWRs, as they are, mostly, lost by wind erosion (Fig. 5).

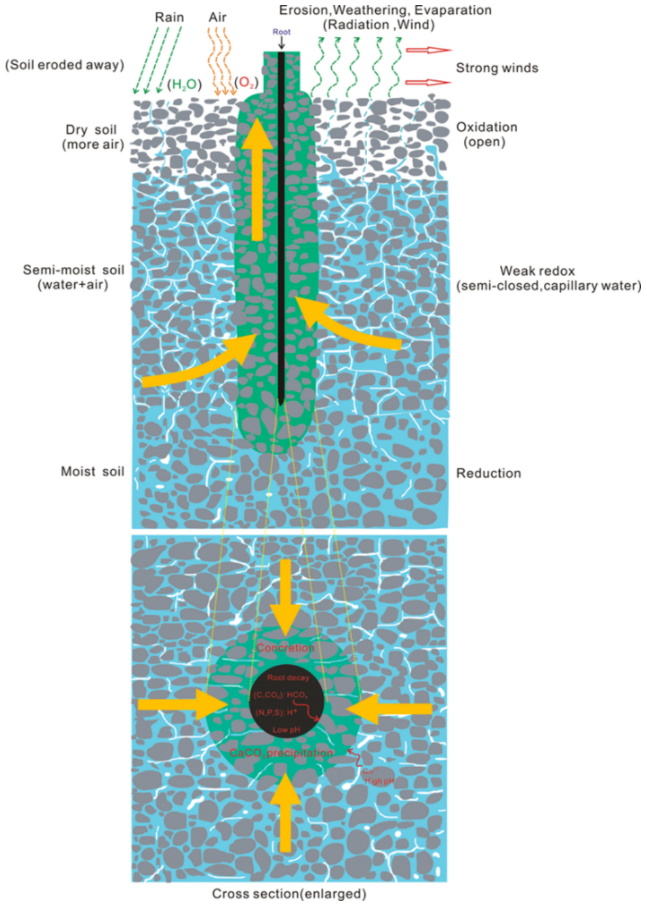

Fig. 5 Conceptual diagram showing formation mechanism of the IR in dune sandy soils. After root death, rhizolith formation starts in semi-closed redox conditions at about 30–50 cm depth below the surface. In these conditions, water is available for chemical reactions (i.e., mineral dissolution and carbonate crystallization) leading to root decomposition, CO_2 release, and mineral dissolution. At the same time, different types of organic acids are produced, inducing a decrease in pH around the root. A steep chemical gradient is generated between the root and surrounding soil. Ca^{2+} ions are released via the dissolution of minerals such as feldspar and lithogenic carbonates. They may later crystallize as calcite around the decomposed roots. At the same time, the channels left after root decomposition provide a conduit for water transportation to the surface, leading then to evaporation and further carbonate precipitation in the channel and/or around the decomposed root relicts. The water transportation to the surface (thick yellow arrows) is due to extreme weather conditions in deserts such as strong winds and solar irradiation. The rhizoliths can be preserved in underground soil. Then, wind may remove the surface soil layer and expose the rhizoliths on the surface. The latter can become thinner and thinner by chemical and mechanical erosion and weathering on the soil surface, and at last broken, lying on the surface

6 Conclusions

The field observations and laboratory analyses of rhizoliths from dune soils of Badain Jaran Desert constrain the main factors influencing their formation:

a. Vegetation type. This is the first key factor for rhizolith formation in this area as the rhizoliths are only formed around the modern dead roots of *Artemisia* rather than roots of any other species such as *Psammochloa villosa* (Trin.) Bor, and *Phragmites Australis*.
b. Soil moisture. Rhizoliths are only present in moist, deeper soil horizons of the dune swales. These sandy soils with suitable water content provide weak oxidation-reduction conditions for gas exchange as well as water migration and evaporation leading to continuous root decomposition, solutes transport, and calcification.
c. Topographic position. Soil pore-water migrates from upper parts of dunes to swales and depressions, where rainfall and dune condensation water is collected. Water is permanently available for *Artemisia* growth in soils of swales and depressions despite the extreme evaporative condition of the region.
d. High aridity and evaporation potential. The high aridity and evaporation due to strong solar radiation and strong winds favor the condensation and crystallization of dissolved carbonates around roots and the formation of rhizoliths.

The *in-situ* rhizoliths are shown to be formed over a very short time after root death, leading to the incorporation of "old" carbon from lithogenic carbonates (as much as 90% of rhizolith carbonates) into the rhizolith structure (Sun et al. 2019a), as evidenced by the ^{14}C date discrepancies between rhizolith carbonates and organic relicts of the roots. Isotopic analyses also highlighted the effects of the low-density vegetation cover and high rates of evaporation in deserts on ^{13}C and ^{18}O isotopic enrichment of rhizoliths. Altogether, these results show that rhizoliths are the reflection of the soil complex and specific environmental and climatic conditions in which they are formed.

Acknowledgements We highly appreciate the constructive comments from Professor Zhuolun Li. We give our thanks to Professor Ping Ding for radiocarbon dating and isotopic work, Pu Wang and Shiming Zhang for their petrographic and mineralogical work; Wenhui Xue and Wentao Pei for their assistance during field exploration. The authors also acknowledge Professor Eric Verrecchia, Professor Xin Wang, Professor Yinglong Chen, Professor Zhiqiang Lei, and Dr. Keyu Fa for their comments. The research was supported by the Natural Science Foundation of China (41561046), Chinese-German Centre (Sino-German Mobility M-0069) and the German Research Foundation (DFG) (ZA 1068/4-1).

Funding Open Access funding enabled and organized by Projekt DEAL.

Availability of data and material All data generated and analyzed during this study are included in this published article.

Declarations

Conflict of interest On behalf of all authors, the corresponding author states that there is no conflict of interest.

References

Albalasmeh AA, Ghezzehei TA (2014) Interplay between soil drying and root exudation in rhizosheath development. Plant Soil 374:739–751

Alonso-Zarza AM (2018) Study of a modern calcrete forming in Guadalajara, Central Spain: An analogue for ancient root calcretes. Sediment Geol 373:180–190

Amundson RG, Chadwick OA, Sowers JM, Doner HE (1989) The stable isotope chemistry of pedogenic carbonates at Kyle Canyon, Nevada. Soil Sci Soc Ame J 53:201–210

Bai Y (2011) Internal structure and formation process of mega-dunes in the Badain Jaran Desert (in Chinese with English abstract). Doctoral dissertation. Lanzhou University. 79–85

Barta G (2011) Secondary carbonates in loess-paleosoil sequences: A general review. Open Geosci 3:129–146

Basum S, Agrawal S, Sanyal P, Mahato P, Kumar S, Sarkar A (2015) C isotopic ratios of modern C_3-C_4 plants from the gangetic plain, India and its implications to paleovegetational reconstruction. Palaeogeo Palaeoclim Palaeoecol 440:22–32

Bayat O, Karimzadeh H, Eghbal MK, Karimi A, Amundson R (2018) Calcic soils as indicators of profound Quaternary climate change in eastern Isfahan. Iran Geoderma 315:220–230

Bloom PR, Nater EA (1991) Kinetics of dissoluton of oxide and primary silicate minerals. Rates of Soil Chemical Processes, Special Publication (Soil Science Society of America), pp 151–189

Bojanowski MJ, Jaroszewicz E, Košir A, Łoziński M, Marynowski L, Wysocka A, Derkowski A (2016) Root-related rhodochrosite and concretionary siderite formation in oxygen-deficient conditions induced by a groundwater table rise. Sediment 63:523–551

Brazier J-M, Schmitt A-D, Gangloff S, Pelt E, Gocke MI, Wiesenberg G, L.B (2020) Multi-isotope approach ($\delta^{44/40}$Ca, $^{88/86}$Sr and ^{87}Sr/^{86}Sr) provides insights into rhizolith formation mechanisms in terrestrial sediments of Nussloch (Germany). Chem Geol 545:119641. https://doi.org/10.1016/j.chemgeo.2020.119641

Cerling TE (1984) The stable isotopic composition of modern soil carbonate and its relationship to climate. Earth and Planet Sci Lett 71:229–240

Cerling TE, Quade J (1993) Stable carbon and oxygen isotopes in soil carbonates. Geophy. Monograph Ser. (Washington DC, American Geophysical Union) 78, 217–231

Chen J, Zhao X, Wang J, Gu W, Sheng X, Su Z (2004) Meaning of the discovery of lacustrine tufa and root-shaped nodule in Badain Jaran Desert for the study on lake recharge(In Chinese with English abstract). Carsol Sinica 432:459–460

Chorover J, Kretzschmar R, Garcia-Pichel F, Sparks DL (2007) Soil Biogeochem Processes within Crit Zone Elem 3(5):321–326

Cohen AS (1982) Paleoenvironments of root casts from the Koobi Fora Formation, Kenya. J Sediment Res 52:401–414

Cramer M, Hawkins HJ (2009) A physiological mechanism for the formation of root casts. Palaeogeo Palaeoclim Palaeoecol 274:125–133

Der Hoven SJ, Quade J (2002) Tracing spatial and temporal variations in the sources of calcium in pedogenic carbonates in a semiarid environment. Geoderma 108(3):259–276

Dickson J (1966) Carbonate identification and genesis as revealed by staining. J Sediment Res 36:491–505

Dong Z, Qian G, Lv P, Hu G (2013) Investigation of the sand sea with the tallest dunes on Earth: China's Badain Jaran Sand Sea. Earth-Sci Rev 120:20–39

Dong Z, Wang T, Wang X (2004) Geomorphology of the megadunes in the Badain Jaran Desert. Geomorphology 60:191–203

Dontsova K, Balogh-Brunstad Z, Chorover J (2020) Plants as drivers of rock weathering. In Biogeochemical Cycles (eds. K. Dontsova, Z. Balogh-Brunstad and G. Le Roux). Biogeochemical Cycles: Ecological Drivers and Environmental Impact, Geophysical Monograph 251, First Edition. American Geophysical Union. John Wiley & Sons, Inc

Dwivedi D, Riley WJ, Torn MS, Spycher N, Maggi F, Tang JY (2017) Mineral properties, microbes, transport, and plant-input profiles control vertical distribution and age of soil carbon stocks. Soil Biol Biochem 107:244–259

Dworkin S, Nordt L, Atchley S (2005) Determining terrestrial paleotemperatures using the oxygen isotopic composition of pedogenic carbonate. Earth Planet Sci Lett 237:56–68

FAO (Food and Agriculture Organization of the United Nations) (2014) World reference base for soil resources. International soil classification system for naming soils and creating legends for soil maps

Gates J, Edmunds M, Darling G, Ma J, Pang Z, Young A (2008) Conceptual model of recharge to southeastern Badain Jaran Desert groundwater and lakes from environmental tracers. Appl Geochem 23:3519–3534

Gao S, Chen W, Jin H, Dong G, Li B, Yang G, Liu L, Guan Y, Sun Z, Jin J (1993) Preliminary study on the Holocene desert evolution in the NW boundary of the Asia monsoon (in Chinese). Sci China Ser D 23:203

Gastaldo RA, Demko TM (2011) The relationship between continental landscape evolution and the plant-fossil record: long term hydrologic controls on preservation, Taphonomy. Springer, pp 249–285

Gocke M, Gulyás S, Hambach U, Jovanović M, Kovács G, Marković SB, Wiesenberg GL (2014) Biopores and root features as new tools for improving paleoecological understanding of terrestrial sediment-paleosol sequences. Palaeogeo Palaeoclim Palaeoecol 394:42–58

Gocke M, Kuzyakov Y, Wiesenberg GL (2010) Rhizoliths in loess–evidence for post-sedimentary incorporation of root-derived organic matter in terrestrial sediments as assessed from molecular proxies. Org Geochem 41:1198–1206

Gocke M, Pustovoytov K, Kühn P, Wiesenberg GL, Löscher M, Kuzyakov Y (2011) Carbonate rhizoliths in loess and their implications for paleoenvironmental reconstruction revealed by isotopic composition: δ^{13}C, ^{14}C. Chem Geol 283:251–260

Golubtsov VA, Khokhlova OS, Cherkashina AA (2019) Carbonate rhizoliths in dune sands of the Belaya River valley (Upper Angara Region). Eurasian Soil Sci 52:83–93

Gudbrandsson S, Wolff-Boenisch D, Gislason SR, Oelkers EH (2014) Experimental determination of plagioclase dissolution rates as a

function of its composition and pH at 22ºC. Geochim Cosmochim Acta 139:154–172
Hinsinger P, Plassard C, Tang C, Jaillard B (2003) Origins of root-mediated pH changes in the rhizosphere and their responses to environmental constraints: A review. Plant Soil 248(1–2):43–59
Holdren GR, Speyer PM (1985) Reaction rate-surface area relationships during the early stages of weathering—I. Initial observations. Geochim Cosmochim Acta 49:675–681
Huguet A, Bernard S, Khatib R, Gocke E, Wiesenberg MI, Derenne GLB, S (2020) Multiple stages of plant root calcification deciphered by chemical and micromorphological analyses. Geobio 00:1–12. https://doi.org/10.1111/gbi.12416
Jiao JJ, Zhang X, Wang X (2015) Satellite-based estimates of groundwater depletion in the Badain Jaran Desert. Chin Sci Rep 5:8960
Jones DL, Nguyen C, Finlay RD (2009) Carbon flow in the rhizosphere: Carbon trading at the soil–root interface. Plant Soil 321(1–2):5–33
Joseph S, Thrivikramaji K (2005) Rhizolithic calcrete in Teris, southern Tamil Nadu: Origin and paleoenvironmental implications. J Geol Soci India 65:158–168
Kolchugin A, Immenhauser A, Walter B, Morozov V (2016) Diagenesis of the palaeo-oil-water transition zone in a Lower Pennsylvanian carbonate reservoir: Constraints from cathodoluminescence microscopy, microthermometry, and isotope geochemistry. Mar Petrol Geol 72:45–61
Kraus MJ, Hasiotis ST (2006) Significance of different modes of rhizolith preservation to interpreting paleoenvironmental and paleohydrologic settings: examples from Paleogene paleosols, Bighorn Basin, Wyoming, USA. J Sediment Res 76:633–646
Lambers H, Mougel C, Jaillard B, Hinsinger P (2009) Plant-microbe-soil interactions in the rhizosphere: An evolutionary perspective. Plant Soil 321(1):83–115
Li C, Yang X (2004) Comparative studies of the climatic indicators inferred from aeolian sediments in the desert regions of northern China (in Chinese with English abstract). Quat Sci 24:469–473
Li Z, Gao Y, Han L (2017) Holocene vegetation signals in the Alashan Desert of northwest China revealed by lipid molecular proxies from calcareous root tubes. Quat Res 88:60–70
Li Z, Wang Na, Cheng H, Ning K, Zhao L, Li R (2015a) Formation and environmental significance of late Quaternary calcareous root tubes in the deserts of the Alashan Plateau, northwest China. Quat Int 372:167–174
Li Z, Wang Na, Li R, Ning K, Cheng H, Zhao L (2015b) Indication of millennial-scale moisture changes by the temporal distribution of Holocene calcareous root tubes in the deserts of the Alashan Plateau, Northwest China. Palaeogeo Palaeoclim Palaeoecol 440:496–505
Li ZL, Wang NA, Li RL, Ning K, Cheng HY, Zhao LQ (2015) Indication of millennial-scale moisture changes by the temporal distribution of Holocene calcareous root tubes in the deserts of the Alashan Plateau, Northwest China. Palaeogeogr Palaeoclimatol Palaeoecol 440:496-505. https://doi.org/10.1016/j.palaeo.2015.09.023
Liang Z, Elsgaard L, Nicolaisen MH, Kjærbye AL, Olesen JE (2018) Carbon mineralization and microbial activity in agricultural topsoil and subsoil as regulated by root nitrogen and recalcitrant carbon concentrations. Plant Soil 433:65–82
Liutkus CM (2009) Using petrography and geochemistry to determine the origin and formation mechanism of calcitic plant molds; rhizolith or tufa? J Sediment Res 79:906–917
Liu XZ, Zhang Y, Li ZG, Feng T, Su Q, Song Y (2017) Carbon isotopes of C3 herbs correlate with temperature on removing the influence of precipitation across a temperature transect in the agro-pastoral ecotone of northern China. Ecol Evol 7(24):10582-10591. https://doi.org/10.1002/ece3.3548
Liutkus CM, Wright JD, Ashley GM, Sikes NE (2005) Paleoenvironmental interpretation of lake-margin deposits using δ13C and δ18O results from early Pleistocene carbonate rhizoliths, Olduvai Gorge. Tanzan Geol 33:377–380
Ma J, Edmunds WM (2006) Groundwater and lake evolution in the Badain Jaran Desert ecosystem, Inner Mongolia. Hydrogeol J 14:1231–1243
Ma N, Wang N, Zhao L, Zhang Z, Dong C, Shen S (2014) Observation of mega-dune evaporation after various rain events in the hinterland of Badain Jaran Desert (in Chinese). Chin Sci Bull 59:162–170
Ma YD, Zhao JB, Zhou Q, Luo XQ, Shao TJ, Yue DP (2017) Identification of runoff type and an assessment of water balance for the megadune area of the Badain Jaran Desert. Environ Earth Sci 76:424
Marschner H (1995) Mineral nutrition of higher plants. Academic Press Limited, London, UK, pp 229–312. http://dx. doi. org/10.1016/B978
Mavris C, Götze J, Plötze M, Egli M (2012) Weathering and mineralogical evolution in a high Alpine soil chronosequence: A combined approach using SEM–EDX, cathodoluminescence and Nomarski DIC microscopy. Sediment Geol 280:108–118
McLaren S (1995) Early carbonate diagenetic fabrics in the rhizosphere of late Pleistocene aeolian sediments. J Geol Soci 152:173–181
Monger HC (2014) Soils as Generators and Sinks of Inorganic Carbon in Geologic Time. In Soil Carbon,Springer International Publishing.27–36
Monger HC, Kraimer RA, Khresat S, Cole DR, Wang X, Wang J (2015) Sequestration of inorganic carbon in soil and groundwater. Geology 43(5):375–378
Nascimento DL, Batezelli A, Ladeira FSB (2019) The paleoecological and paleoenvironmental importance of root traces: Plant distribution and topographic significance of root patterns in Upper Cretaceous paleosols. Catena 172:789–806
Omer MF, Omer D, Zebari BG (2014) High resolution cathodoluminescence spectroscopy of carbonate cementation in Khurmala Formation (Paleocene – L. Eocene) from Iraqi Kurdistan Region, Northern Iraq. J Afr Earth Sci 100:243–258
Owen RA, Owen RB, Renaut RW, Scott JJ, Jones B, Ashley GM (2008) Mineralogy and origin of rhizoliths on the margins of saline, alkaline Lake Bogoria, Kenya Rift Valley. Sediment Geol 203:143–163
Omer MF (2015) Cathodoluminescence petrography for provenance studies of the sandstones of Ora Formation (Devonian-Carboniferous), Iraqi Kurdistan Region, northern Iraq. J Afr Ear Sci 109:195-210. https://doi.org/10.1016/j.jafrearsci.2015.05.021
Quade J (2014) The carbon, oxygen, and clumped isotopic composition in soil carbonate archeology, Treat. Geoche. 129–143
Rao VP, Thamban M (1997) Dune associated calcretes, rhizoliths and paleosols from the western continental shelf of India. Oceano Lit Rev 11:1273
Rasse DP, Rumpel C, Dignac M (2005) Is soil carbon mostly root carbon? Mechanisms for a specific stabilisation. Plant Soil 269(1):341–356
Reimer P, Austin WEN, Bard E, Bayliss A, Blackwell PG, Ramsey B, Butzin C, Cheng M, Edwards HLawrence, Friedrich R, Grootes M, Guilderson PM, Hajdas TP, Heaton I, Hogg TJ, Hughen AG, Kromer KA, Manning B, Muscheler SW, Talamo R, S (2020) The IntCal20 Northern Hemisphere radiocarbon age calibration curve (0–55 cal kBP). Radiocarbon 62(4):725–757. https://doi.org/10.1017/RDC.2020.41
Sanaullah M, Chabbi A, Leifeld J, Bardoux G, Billou D, Rumpel C (2011) Decomposition and stabilization of root litter in top- and subsoil horizons: What is the difference? Plant Soil 338(s1–2):127–141

Sarjeant WAS (1975) Plant trace fossils. The study of trace fossils: A ynthesis of principles, problems, and procedures in ichnology, 163–179

Scholonek C, Augustsson C (2016) Can cathodoluminescence of feldspar be used as provenance indicator? Sediment. Geol 336:36–45

Shao TJ, Zhao JB, Dong ZB (2015) Grain-size distribution of the aeolian sediment and its effect on the formation and growth of mega-dunes in the Badain Jaran Desert, northwest China. Z für Geomorphologie 59:273–286

Shen CD, Ding P, Wang N (2010) Buried ancient forest and implications for paleoclimate since the mid-Holocene in South China. Radiocarbon 52:1411–1421

Smith FA, White JWC (2004) Modern calibration of phytolith C isotope signatures for C_3/C_4 paleograssland reconstruction. Paleogeogr Paleoclimatol Paleoecol 207:277–304

Smits MM, Hoffland E, Jongmans AG, Van Breemen N (2005) Contribution of mineral tunneling to total feldspar weathering. Geoderma 125(1):59–69

Spohn M, Ermak A, Kuzyakov Y (2013) Microbial gross organic phosphorus mineralization can be stimulated by root exudates– A33P isotopic dilution study. Soil Biol Biochim 65:254–263

Sun QF, Zamanian K, Huguet A, Fa KY, Wang H (2020) Characterization and formation of the pristine rhizoliths around *Artemisia* roots in dune soils of Tengeri Desert, NW China. Catena 193 (2020) 104633

Sun QF, Wang H, Zamanian K (2019a) Radiocarbon age discrepancies between the carbonate cement and the root relics of rhizoliths from the Badain Jaran and the Tengeri deserts, Northwest China. Catena 180:263–270

Sun Q, Xue W, Zamanian K, Colin C, Duchamp-Alphonse S, Pei W (2019b) Formation and paleoenvironment of rhizoliths of Shiyang river basin, Tengeri Desert, NW China. Quat Int 502:246–257

Van Breemen N, Mulder J, Driscoll CT (1983) Acidification and alkalinization of soils. Plant Soil 75(3):283–308

Vogel JC (1993) Variability of carbon isotope fractionation during photosynthesis. In: Ehleringer JR, Hall AE, Farquhar GD (eds) Stable isotopes and plant carbon–water relations. Academic Press, San Diego, CA, pp 29–38

Wang Y, Cao J, Zhang X, Shen Z, Mei F (2004) Carbonate content and carbon and oxygen isotopic composition of surface soil in the dust source regions of China (In Chinese with English abstract). Mar Geol and Quat Geol 24:113–117

Welch S, Ullman W (1996) Feldspar dissolution in acidic and organic solutions: Compositional and pH dependence of dissolution rate. Geochim Cosmochim Acta 60:2939–2948

Xu X, Trumbore SE, Zheng S, Southon JR, McDuffee KE, Luttgen M, Liu JC (2007) Modifying a sealed tube zinc reduction method for preparation of AMS graphite targets: reducing background and attaining high precision. Nucl Instrum Methods Phys Res Sect B 259:320–329

Yang X (2000) Landscape evolution and precipitation changes in the Badain Jaran Desert during the last 30 000 years. Chin Sci Bull 45:1042–1047

Yang X, Liu T, Xiao H (2003) Evolution of megadunes and lakes in the Badain Jaran Desert, Inner Mongolia, China during the last 31,000 years. Quat Int 104(1):99–112

Yang X, Ma N, Dong J, Zhu B, Bing X, Ma Z et al (2010) Recharge to the interdune lakes and Holocene climatic changes in the Badain Jaran desert, Western China. Quat Res 73(1):10–19

Yang X, Scuderi L, Liu T, Paillou P, Li H, Dong J, Zhu B, Jiang W, Jochems A, Weissmann G (2011) Formation of the highest sand dunes on Earth. Geomorphology 135:108–116

Yuan G, Cao Y, Schulz HM, Hao F, Gluyas J, Liu K, Yang T, Wang Y, Xi K, Li F (2019) A review of feldspar alteration and its geological significance in sedimentary basins: From shallow aquifers to deep hydrocarbon reservoirs. Earth-Sci Rev 191:114–140

Zamanian K, Pustovoytov K, Kuzyakov Y (2016) Pedogenic carbonates: forms and formation processes. Earth-Sci Rev 157:1–17

Zhang K, Cai D, Ao Y, An Z, Guo Z (2017) Local Circulation Maintains the Coexistence of Lake-dune Pattern in the Badain Jaran Desert. Sci Rep 7:1–5

Zhao X, Zhao C, Stahr K, Kuzyakov Y, Wei X (2020) The effect of microorganisms on soil carbonate recrystallization and abiotic CO_2 uptake of soil. Catena 192:104592

Kazem, Zamanian Alex R., Lechler Andrew J., Schauer Yakov, Kuzyakov Katharine W., Huntington (2021) Quat Res 101256-272 10.1017/qua.2020.109

Kazem, Zamanian Konstantin, Pustovoytov Yakov, Kuzyakov (2016) Cation exchange retards shell carbonate recrystallization: consequences for dating and paleoenvironmental reconstructions. Catena 142134-138 10.1016/j.catena.2016.03.012

Kazem, Zamanian Konstantin, Pustovoytov Yakov, Kuzyakov (2016) Recrystallization of shell carbonate in soil: 14 C labeling modeling and relevance for dating and paleo-reconstructions. Geoderma 28287-95 10.1016/j.geoderma.2016.07.013